

# Spectroscopic Investigation of Companion Stars in Herbig AeBe Binary Systems

A. Sweet<sup>1</sup>

*Department of Physics and Astronomy, Macalester College, St. Paul, MN 55105*

`asweet@macalester.edu`

G. Doppmann and B. Rodgers

*Gemini Observatory - South, La Serena, Chile*

## ABSTRACT

Herbig AeBe (HAEBE) binary systems are good environments for the study of pre-main sequence stellar evolution in companion stars whose mass may be significantly lower than that of the primary star. Measurements of the spectral type and surface gravity of the companion star in the system allow it to be placed on the H-R diagram, where theoretical evolutionary model tracks can then constrain its mass and age, and comparisons can be made between these low mass stars and those formed without the presence of a high mass star. Because of the extinction associated with objects in star forming regions, the near-infrared offers a less obscured wavelength region than the optical through which to study these objects. Medium (R= 1,700 & 6,000) and High (R=18,000) Resolution near infrared (NIR) spectra were gathered for the analysis of these companion stars. We present two different ways to measure  $T_{eff}$  and estimate  $\log g$  from the spectra of late type stars, depending on the spectral resolution. At high resolution, detailed model fits to the shapes of Na lines at  $2.21 \mu\text{m}$  and the (2-0)  $^{12}\text{CO}$  bandhead at  $2.29 \mu\text{m}$  provides an accurate way to measure effective temperature ( $\sigma = 190 \text{ K}$ ) and surface gravity ( $\sigma = 0.82 \text{ cm s}^{-2}$ ), in addition to allowing for values of  $v \sin i$ , veiling, and radial velocity to be estimated. At medium resolution, the equivalent widths of 10 of the strongest absorption lines present in the NIR spectrum were measured to determine  $T_{eff}$  at a lower accuracy. Preliminary results show that these techniques are effective for characterizing late-type companions. Analysis of two stars is discussed, more data is needed to address statistical questions about the nature of HAEBE companions.

*Subject headings:* NIR spectroscopy, binary systems, HAeBe companion stars

---

<sup>1</sup>CTIO REU 2006 participant

## 1. Introduction

While the stellar evolution of main sequence stars is well understood, that of pre-main sequence (PMS) objects is not. HAEBE stars are one group of PMS stars classified by George Herbig in 1960 (1) during his search for the higher mass equivalent to the low mass T Tauri stars. These Herbig stars cover a wide range of intermediate masses, usually between 2-8  $M_{\odot}$ , have spectral types between B-F, are associated with a star forming region, and show some IR-excess or emission lines. Current published catalogues (The et al. 1994, Malfait et al. 1998, Acke et al. 2004, Acke et al. 2005) list over 280 stars as candidate objects with more unpublished data further increasing this number (Bouvier et al. preprint).

HAEBE stars are often found in groups and thus these environments are important, not only because binary fraction is critical for the Initial Mass Function but also because the study of star formation of more massive stars offers insight into stellar evolution as a function of mass. In addition, learning the properties of stellar evolution of a less massive star in the presence of a higher mass star lends insight into the effect of environment on stellar formation (Hillenbrand et al. 1992). Finally, in binary systems there is the possibility of a dynamical mass measurements, which can test theoretical evolutionary model tracks as well as providing a way to calibrate systematic errors in converting  $T_{eff}$  and  $\log g$  into mass and age.(Doppmann et al. 2003)

Specifically, in this work we are interested in the effects that a more massive PMS Herbig star has on the environment and evolution of its low mass companion, in addition to learning about PMS stellar evolution across a wide range in mass. By classifying the spectral type of the companion star, we will be able to place the companion on an H-R diagram in order to say something about its evolution. (Rodgers, observing proposal 2006)

One reason HAEBE stars are poorly understood is because they are a small, heterogenous sample of stars located over a large range in distance and with a greater probability of occurring in binary or multiple systems than as isolated objects. However, despite the difficulty of making statistical conclusions, the spatial and spectral heterogeneity of the sample along with the presence of companions that may be of a significantly different spectral type make these objects well-suited for drawing conclusions about star formation as a function of mass. Previous photometric studies have shed some light on the properties of these objects, requiring corrections for extinction. Now with sensitive IR spectrographs on large aperture telescopes, more accurate measurements of the star and disk properties can be made through a detailed spectroscopic analysis (Doppmann et al. 2003, Hernandez et al. 2004). At high resolution, where absorption lines are fully resolved, the star's effective temperature, surface gravity,  $v \sin i$  rotation, radial velocity and the amount of continuum veiling from the surrounding disk alter the line shapes, allowing these effects to be measured without any dependence on the absorption by intervening material. Even at lower spectral resolution, line equivalent widths are not dependent on extinction, and the effects of continuum veiling (i.e. the addition of infrared emission presumably due to the disk) can also be estimated.

The optimal waveband, and indeed the most effective, through which to view these types of

objects is the near infrared (NIR). The use of longer wavelengths makes viewing objects surrounded by dust and gas easy to view without considerable correction for extinction, yet the wavelengths are still short enough to be sensitive to the lines in the stellar photosphere, making stellar observations straightforward without extra information from the warm thermal emission of the circumstellar disk. Finally, this wavelength region avoids the accretion shock emission and continuum excess which can overwhelm the spectra in the optical and UV bands (Doppmann et al. 2003, Hernandez et al. 2004)

## 2. Data

### 2.1. Sample selection

Stars were chosen to be the known binary companion to a Herbig star, with a binary separation greater than  $0.8''$ , the limiting spatial resolution of the Gemini Near Infrared Spectrograph (GNIRS).

### 2.2. Observations

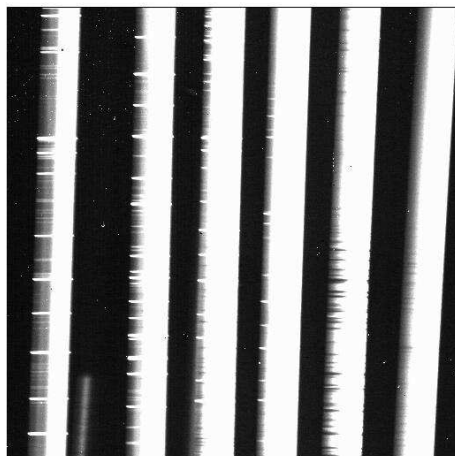


Fig. 1.— An example image of a raw, unreduced, cross-dispersed spectra of an object from the Gemini GNIRS instrument.

Near-IR spectra of the sample stars were acquired on 2005 April 20 and 2005 October 10 UT, and spectra of the MK spectral standards was acquired between 2005 November 21 – 23 UT. All data were collected using the 8.1 m Gemini-South telescope in Chile using GNIRS. For the standard stars, the 111 1/mm grating was used with the long camera at central wavelengths of 2.21 and 2.29

$\mu\text{m}$  and slit width of 0.1" providing data of spectroscopic resolution of  $R \equiv \lambda/\delta\lambda = 18,000$ . Three different configurations were used to collect data from the different targets. For HR5999B, the 111 1/mm grating was used with the long camera and central wavelength of 2.19  $\mu\text{m}$  and a slit width of 0.1" for a resolution of  $R = 18,000$ . For BF Ori B, and S Mon A and B (refer to figure 1 for an example unreduced spectra), the 111 1/mm grating was used with the short camera and a central wavelength of 1.63  $\mu\text{m}$  and a slit width of 0.3" in cross-dispersed mode to yield a resolution of  $R = 6,000$ . Finally, for CO Ori A and B, the 32 1/mm grating was used with the short camera in cross dispersed mode and a central wavelength of 1.65  $\mu\text{m}$  and a slit width of 0.3" for a resolution of  $R = 1,800$ . The lower resolution data provides more spectral coverage providing more lines for investigation. The lowest resolution data covers the entire 0.8-2.5  $\mu\text{m}$  spectral range. The central wavelengths were chosen to optimize the number of features used for spectral type identification in addition to the important common emission lines. Flats, arcs and spectra of hot telluric standards were also taken.

### 2.3. Data Reduction

All data were reduced following standard procedures with IRAF from the Gemini GNIRS package. Frames were flatfield divided and sky subtracted before spectra were extracted. Extracted spectra were wavelength calibrated using lines in arc lamp exposures.

Telluric features were removed by dividing wavelength calibrated object spectra by spectra of early type stars observed at similar airmass and slit position. Spectral orders were corrected for telluric absorption with the use of the XTELLCOR IDL routine developed as part of SpexTool package. This routine creates and then removes a pure telluric spectrum which is generated by dividing an observed early stellar spectrum by a synthetic model of Vega (modified to include line broadening). Combined spectra were then produced by summing the spectra of both slit positions for each object. Finally, the spectra of each wavelength sub-interval used in our analysis, were flattened and continuum normalized to one by linear function, so as to be directly comparable to the intrinsically flat continua of our synthesis models.

## 3. Spectral Analysis

There were two spectral methods utilized to measure stellar properties in our HAeBe sample. Each method used Ames models (Hauschildt 2003, private communication), which are a new sequence of NIR synthesis templates based on local thermodynamic equilibrium radiative transfer through a NEXTGEN stellar atmosphere profile. These models cover the entire near-IR spectral range (0.8  $\mu\text{m}$  - 2.5  $\mu\text{m}$ ) at high resolution ( $R > 10,000$ ) across a range in  $T_{eff}$  (2,000-5,000 K) and  $\log g$  (2.5-5.5  $\text{cm s}^{-2}$ )

The first method was used with our high resolution data ( $R=18,000$ ) by matching spectral

synthesis models to find the best pixel to pixel fit across the absorption lines that were present in the data. The fitting focuses on the sodium lines located at approximately 2.207 & 2.209  $\mu\text{m}$  and the (2-0)  $^{12}\text{CO}$  bandhead located at 2.2935  $\mu\text{m}$ . (Refer to figure 2) We first used this method with the MK standard stars to calibrate the systematic errors in the fitting procedure. The technique was then applied to the source HR5999B, and allowed for a precise temperature,  $v \sin i$  rotation, radial velocity, and continuum veiling measurement (at a fixed gravity) to be made. We also used this technique on the medium resolution data of BF Ori B to compare the results with those of the medium resolution analysis.

The second technique was the application of a qualitative eye-fit to the entire spectrum paying particular attention to the fits between several strong lines in the spectra and the model. (Refer to figure 3) Measurements of the equivalent widths of selected lines were made to quantify the best fit temperature for each of the strongest absorption lines present in the spectra at lower resolution ( $R = 6000$ ). This technique allows for a more comprehensive fit to  $T_{eff}$  and veiling, but without precise kinematic information, and was used briefly on CO Ori A and B (which were too low resolution to draw conclusions, refer to figure 3) and extensively on BF Ori B.

No method could be used with S Mon A or B because after the reduction of the data the spectral types of both stars were discovered to be early type and therefore did not have the absorption lines present at the wavelength to specifically classify the spectral type using these programs.

### 3.1. Fitting Line Shapes: High Resolution

Using the high resolution observations ( $R = 18,000$ ) of the Na and CO spectral features, we can measure the  $T_{eff}$  and  $\log g$  of a star in addition to the measurement of  $v \sin i$  rotation and radial velocity.

To make these comparisons we used an existing technique (Doppmann et al., 2003) to measure the above noted properties in a selection of MK standards for which there were published  $T_{eff}$  and  $\log g$  available in the literature (de Jager et al. 1987). Older models were used for this fitting technique but were later discarded due to an insufficient range in wavelength coverage,  $T_{eff}$  and  $\log g$  (Refer to figures 5 and 6)

We then applied this technique to high resolution data, namely HR5999B. Because only the Na portion of the spectra was available to us we assumed 2 different values for  $\log g$  (3.5 and 4.5) and then fit for  $T_{eff}$ ,  $v \sin i$ , rotational velocity, and veiling (refer to figure 7). In order to correctly constrain the gravity, we need the CO portion of the spectrum, which is an excellent way to constrain these parameters.

As more high resolution data becomes available, we will apply this technique to that data to further determine the degeneracies/errors associated with  $T_{eff}$  and  $\log g$ .

Finally, we applied this method to BF Ori B although it was medium resolution data. It also

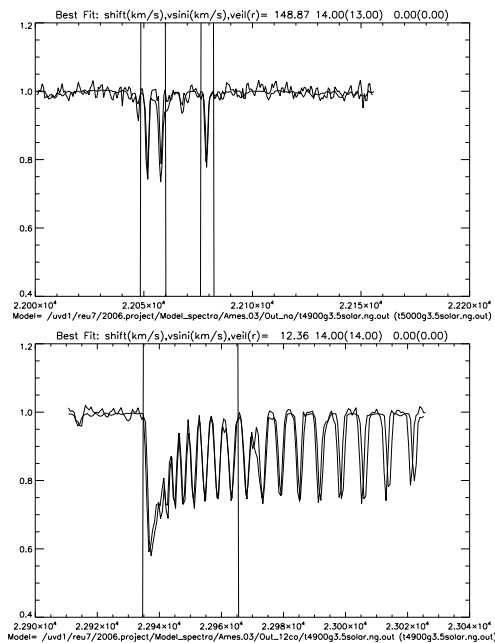


Fig. 2.— An example of the high resolution fitting technique used on the standard star HD74137. Vertical lines denote the region where the RMS is relevant and are fit around the 2.207 & 2.209  $\mu\text{m}$  and the (2-0)  $^{12}\text{CO}$  bandhead located at 2.2935  $\mu\text{m}$ . Refer to table 1 for complete results of fits from standard stars.

only contained the sodium lines so we were unable to constrain  $\log g$ . We chose to analyze this star using this method in order to compare the result with the result gotten from the following medium resolution analysis.

### 3.2. Fitting Line Strengths: Medium Resolution

For the medium resolution data, we identified which objects showed late-type features and selected the 10 strongest absorption features on which to base our spectral analysis (refer to table 2, figure 8). An equivalent width technique developed in this work was used to compare the equivalent widths of the observed lines with those same lines in the Ames models across a range of temperatures and at 2 different  $\log g$  values (3.5, 4.5). Using an IDL program written by G. Doppmann, equivalent widths were measured consistently line by line. This analysis was supplemented by an eye-fit routine showing the best model fits to all of the selecting lines in the 6 cross-dispersed orders.

Like with HR5999B, we assume a fixed gravity, then look for the best fit in  $T_{eff}$ . By examining Figure 9 and 10, conclusions are difficult to draw due to the wide spread of best fit temperatures across the orders and degeneracies in  $T_{eff}$  and  $\log g$ . Although we lack measurement of precise

Table 1: Standard Stars

Star	Spectral Type <sup>a</sup>	$T_{eff}$ <sup>a</sup>	$T_{eff}$ <sup>b</sup>	$T_{eff}$ <sup>c</sup>	$\log(g)$ <sup>a</sup>	$\log(g)$ <sup>b</sup>	$\log(g)$ <sup>c</sup>
HD22049	K2V	5091	4838*	5000	4.61	...	5.5
HD74137	K0III	4620	4655	4870	3.00	...	3.5
HD28	K0III-IV	4710	4715*	5000	2.73	...	3.5
HD66478	K2III	4300	4380*	4480 <sup>+</sup>	2.10 <sup>-</sup>	...	2.5
HD81797	K3III	4383	4256	4280	1.86	...	2.5
HD78541	K4III	3890	4150	4260	1.55	...	2.5
HD80874	M0.5III	3600	3644*	3930 <sup>+</sup>	1.40 <sup>-</sup>	...	2.5
HD57615	M3III	3650	3483	3880 <sup>+</sup>	1.2 <sup>-</sup>	...	2.5

<sup>a</sup>From Cayrel

<sup>b</sup>From DeJager

<sup>c</sup>This work

\*No exact values available;  $T_{eff}$  value estimated from DeJager Spectral Type

<sup>+</sup>No exact values available;  $T_{eff}$  value estimated from values of Cayrel stars of similar spectral type

<sup>-</sup>No exact values available;  $\log g$  value estimated from values of Cayrel stars of similar type

Table 2: Strongest Lines

Element	order	Wavelength ( $\text{\AA}$ )
Na I	8	8183.25
Na I	8	8194.83
Ti I	7	9640.942
Al I	5	13127.03
Al I	5	13154.38
Al I	4	16755.18
Al I	4	16767.95
Al I	4	16723.54
Na I	3	22062.45
Na I	3	22089.69

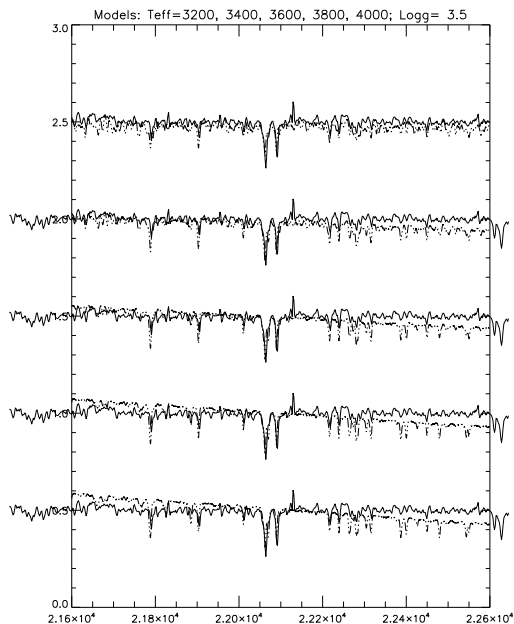


Fig. 3.— An example of the qualitative eye fit plot as part of the medium resolution fitting technique. Plot shows the sodium lines in the third order of the spectra of BF Ori B. The solid line denotes the data, and the dashed line is that of the models. Temperature is greatest at the topmost spectral fit and gets cooler as you move down. Changes in the model line strengths can be seen with the stronger lines.

kinematic information, we can speculate on the veiling. In the case of BF Ori B, the strongest line (Na:  $2.207 \mu\text{m}$ ) suggests veiling is minimal, however this is in disagreement with the other lines. Thus for our analysis, we will use the results obtained by the sodium line fits, as we have the high resolution analysis for this data.

#### 4. Results and Conclusions

Compiling the results from these various techniques (refer to table 3), we can plot these points on an H-R diagram (refer to figure 11) and begin to draw conclusions. While there are errors involved and there is still much to be determined, the preliminary results show that two of our stars are late type and occupy the same region of the graph as the T. Tauri stars (low mass PMS stars formed independently of a high mass companion), which suggests that the low mass stars formed in the presense of a massive star may not be very different from those found alone.

This asks some interesting questions about why these stars have different spectral types. One might expect that stars formed of the same material at the same time in the same region would

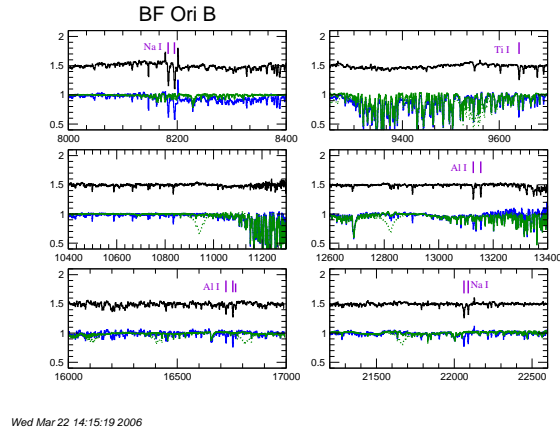


Fig. 4.— An example of the difference in spectra between a hot, early type star (S Mon) and a cooler, late type star (BF Ori B), on which we ran our programs.

look the same but this is not necessary the case. Currently, the body of data shows that about half the companion stars in these systems are early type while the other half are late type. The question still remains what causes this difference, in addition to determining whether there is a correlation between spectral type of the primary and spectral type of the companion. Future work, including the analysis of more stars with high resolution data of both the Na and CO spectral regions as well as the refinement of the medium resolution analysis technique, will hopefully answer some of these questions.

Thank you so much to Greg and Bernadette, my mentors at Gemini from which I learned a great deal about IRAF, IDL, data reduction and of course astronomy in general! Thank you to Stella for being a great REU program director, this has been a wonderful experience. Thank you to the other REU/PIA students for making my time so much fun, and finally, thank you to the NSF for funding the REU program and making this experience possible.

## REFERENCES

- Acke, B., van den Ancker, M. E., 2004 *A&A*, 426, 151-170
- Acke, B., van den Ancker, M. E., Dullemond, C. P., 2005 *A&A*, 436, 209-230
- Bouvier, J., Corcoran, P., Rigaut, F., Tessier, E., Prieur, J.L., Beuzit, J.L., preprint
- de Jager, C. & Nieuwenhuijzen, H. 1987, *A & A*, 177, 217
- Doppmann, G.W., Jaffe, D.T., White, R.J., 2003, *AJ*, 126, 3043-3057

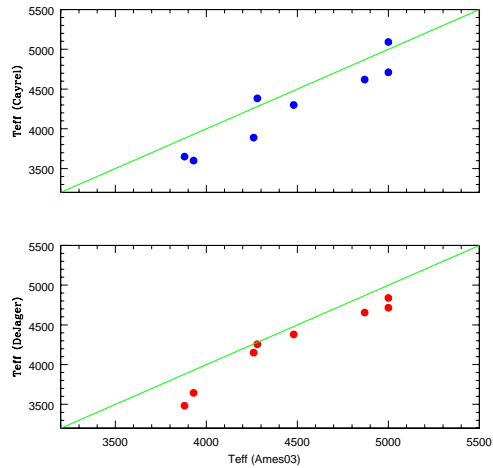


Fig. 5.— Showing the comparison between the derived  $T_{eff}$  of our data sample and the literature values for two different sources as noted. Note the systematic offset.

Herbig, G.H. *ApJS*, 4, 337

Hernandez, J., Calvet, N., Briceno, C., Hartman, L., Berlind, P., 2004, *AJ*, 127, 1682-1701

Hillenbrand, L. A., Strom, S.E., Vrba, F., Keene, J., 1993 *ApJ*, 397, 613-643

Malfait, K., Bogaert, E., Waelkens, C. 1998 *A&A*, 331, 211-223

Rodgers, B. Gemini South Observing Proposal, semester 2006A

The, P.S., de Winter, D., Perez, M.R., 1994 *A&AS*, 104, 315

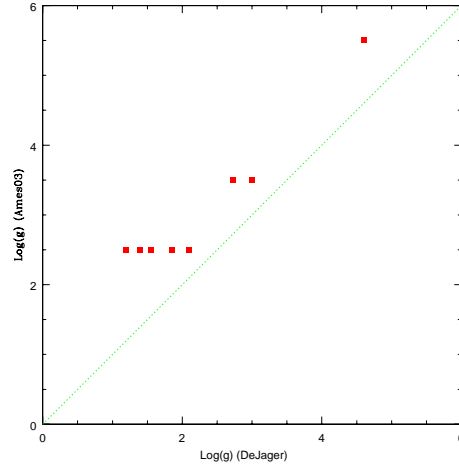


Fig. 6.— Showing the comparison between the derived values of  $\log g$  of our data sample and the literature values. Again, note the offset but keep in mind the limitations of the models.

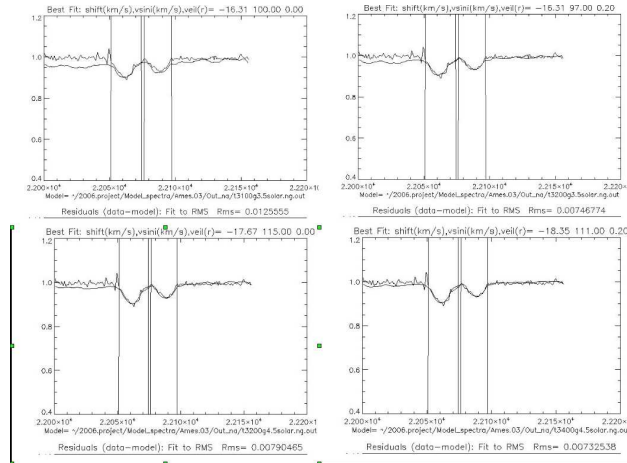


Fig. 7.— Showing the different iterations performed on HR5999B with the values for  $\log g$  changed, and the veiling parameter turned on and off. Best fit shown in the lower righthand corner.

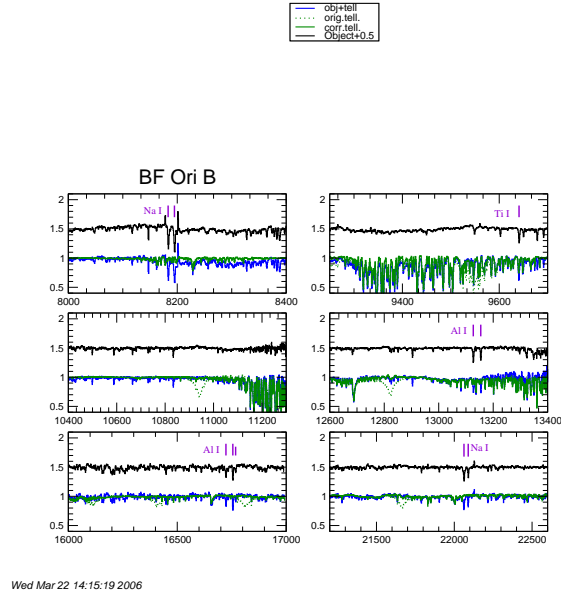


Fig. 8.— Showing the strongest 10 lines marked in the spectrum of BF Ori B.

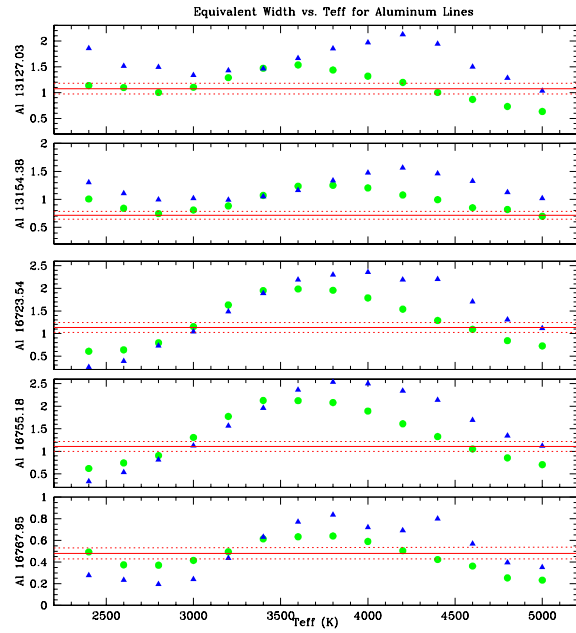


Fig. 9.— Showing the results of the equivalent plots for the Aluminum lines in our spectrum.

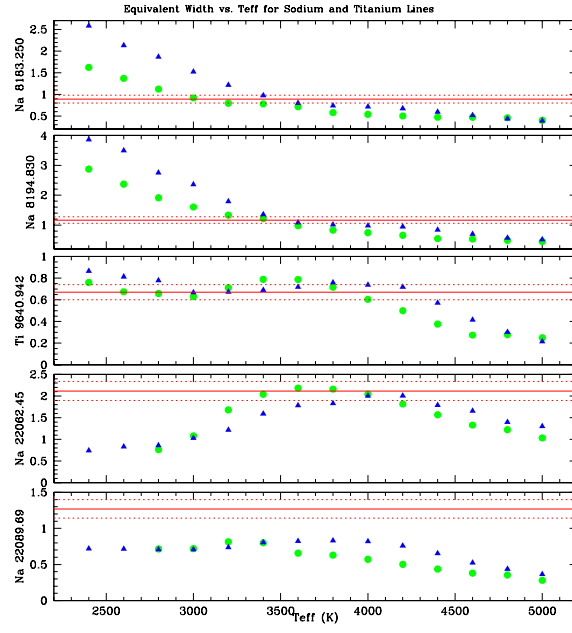


Fig. 10.— Showing the results of the equivalent plots for the Sodium and Titanium lines in our spectrum.

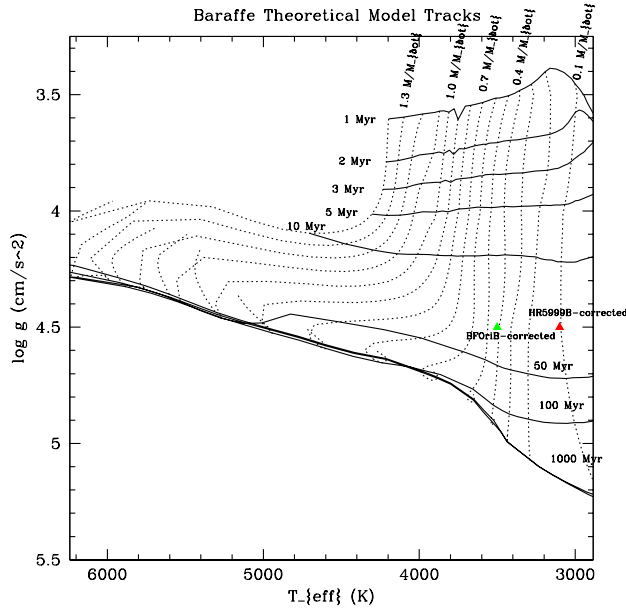


Fig. 11.— Our results for BF Ori B and HR5999 B, corrected for the systematic offset in our fitting techniques. These stars lie in the H-R diagram in the same region that the low mass T Tauri stars do.

Table 3: Raw Results of Spectral Analysis:Uncorrected for Systematic Offset.

Star	Calculated $T_{eff}$	Calculated $\log g$	$v \sin i$	radial velocity	veiling
HR5999 B	3400	4.5	111	-18.35	0.20
S Mon B <sup>a</sup>	...	...	...	...	...
CO Ori A <sup>b</sup>	...	...	...	...	...
CO Ori B <sup>b</sup>	...	...	...	...	...
BF Ori B (high res)	3800	4.5	44	9.51	0.00
BF Ori B (medium res)	3200*	...*	...	...	...

<sup>a</sup>Object early type; no spectral analysis possible

<sup>b</sup>Resolution too low for analysis

\*Analysis inconclusive